

FAST AND STABLE DETERMINISTIC APPROXIMATION OF GENERAL SYMMETRIC KERNEL MATRICES IN HIGH DIMENSIONS

DIFENG CAI*, JAMES NAGY*, AND YUANZHE XI*

Abstract. Kernel methods are used frequently in various applications of machine learning. For large-scale applications, the success of kernel methods hinges on the ability to operate certain large dense kernel matrix K . To reduce the computational cost, Nyström methods can efficiently compute a low-rank approximation to a symmetric positive semi-definite (SPSD) matrix K through landmark points and many variants have been developed in the past few years. For *indefinite* kernels, however, it has not even been justified whether Nyström approximations are applicable. In this paper, we study for the first time, both theoretically and numerically, the Nyström method for approximating general symmetric kernels, including indefinite ones. We first develop a unified theoretical framework for analyzing Nyström approximations, which is valid for both SPSD and indefinite kernels and is *independent* of the specific scheme for selecting landmark points. To address the accuracy and numerical stability issues in Nyström approximation, we then study the impact of data geometry on the spectral property of the corresponding kernel matrix and leverage the discrepancy theory to propose the *anchor net method* for computing Nyström approximations. The anchor net method operates entirely on the dataset without requiring the access to K or its matrix-vector product and scales linearly for both SPSD and indefinite kernel matrices. Extensive numerical experiments suggest that indefinite kernels are much more challenging than SPSD kernels and most existing methods will suffer from numerical instability. Results on various kinds of kernels and machine learning datasets demonstrate that the new method resolves the numerical instability and achieves better accuracy with smaller computation costs compared to the state-of-the-art Nyström methods.

Key words. Nyström method, kernel method, low-rank approximation, error analysis, high-dimensional data

AMS subject classifications. 15A23, 68W25, 11K38, 65D99

1. Introduction. Kernel methods provide a powerful tool for solving nonlinear problems in data science and are used in various machine learning techniques such as support vector machine (SVM), kernel ridge regression, spectral clustering, Gaussian processes (GPs) [5]. Given n data points x_1, \dots, x_n and a kernel function $\kappa(\cdot, \cdot)$, kernel methods form an $n \times n$ kernel matrix $K_{i,j} = \kappa(x_i, x_j)$ to implicitly map data to a kernel feature space, where the originally nonlinear relationship between categories can be transformed into a linear one. The kernel function κ is often taken to be symmetric positive semi-definite (SPSD) in the literature [34]. Recently, methods based on indefinite kernel functions such as jittering kernel [10], Kullback-Leibler divergence kernel [24], tangent distance kernel [16] and multiquadric kernel [13] have also been developed. In addition, indefinite kernel matrices also occur as the derivatives of SPSD kernels in solving optimization problems (see, for example [4]). Theoretical justifications for the support vector machines associated with indefinite kernels can be found in [29, 15].

Due to the need to assemble and operate dense kernel matrices K , kernel methods are often quoted to scale at least $O(n^2)$. For SPSD kernels, a popular approach to circumvent this computational bottleneck is to work with a low-rank approximation to K . Nyström methods are widely used to derive low-rank approximations to kernel matrices. It computes the low-rank factors by constructing a small subset of points, known as *landmark points*. The original Nyström method in [36] selects

*Department of Mathematics, Emory University, Atlanta, GA 30322 (dcai7@emory.edu, jnagy@emory.edu, yxi26@emory.edu). The research of Difeng Cai and Yuanzhe Xi are supported by NSF award OAC 2003720 and the research of James Nagy is supported by NSF award DMS 1819042.

landmark points via a uniform sampling over the dataset, and is often called the uniform Nyström method. Later, non-uniform sampling techniques have been proposed to improve the approximation accuracy [20, 1, 14, 26]. Although extensive studies have been performed to provide the statistical guarantees for these non-uniform sampling schemes [20, 1, 14, 26], most methods cost at least $O(n^2)$ to compute the sampling probability, which prevent them from being explored for solving large-scale problems. Recently, several new developments alleviate this issue with a divide-and-conquer approach and achieve a good balance between the computational efficiency and approximation accuracy [26, 32]. In addition to the probabilistic Nyström methods, a clustering-based method was proposed in [38, 37]. A comprehensive comparison among different sampling and the k -means clustering Nyström methods can be found in [20]. Another widely adopted class of low-rank approximation approaches for SPSD kernels is known as random kitchen sinks (or random Fourier features method) [30, 31, 22]. It expresses the kernel function as an expectation (an integral essentially) via the Fourier transform and then applies sampling to derive low-rank approximations. It was observed in [26] that random kitchen sinks are faster but not as accurate as Nyström methods.

Despite the success of Nyström methods for SPSD kernels in machine learning, to the best of our knowledge, there is *no* discussion on the applicability of Nyström methods for *indefinite* kernels. Note that error estimates that rely on either Cholesky decomposition or ridge leverage scores are no longer valid for indefinite kernels. Therefore, one of the main motivations of this paper is to develop a theoretical framework for analyzing the Nyström approximation error that is applicable to both SPSD and indefinite kernel matrices. Computationally, indefinite kernel matrices are more likely to cause numerical stability issues since regularization is no longer effective when computing the matrix pseudoinverse in the Nyström formula. Therefore, when dealing with indefinite kernels, it is of great importance to design a Nyström scheme, or essentially a landmark points selection scheme, that avoids the possible numerical breakdown. To obtain a robust Nyström approximation, we exploit the relation between data geometry and the numerical rank of the corresponding kernel matrix. The main contributions of the paper are summarized as follows.

1. **Universal Nyström error estimate.** To analyze the Nyström approximation error, we present a theoretical framework that is *universal* in the following sense: (1) it is valid for both SPSD and indefinite kernel matrices; (2) it is independent of the underlying scheme to generate the landmark points. One major theoretical result of the paper is a *computable, method-independent, kernel-independent, deterministic* error bound for Nyström approximation in the following form:

$$(1.1) \quad \max_{i,j} |E_{ij}| \leq \epsilon_1 + 2\epsilon_2 + C_S \epsilon_2^2,$$

where E is the difference between the exact kernel matrix and its Nyström approximation, ϵ_1, ϵ_2 are *computable* quantities, and C_S is the norm of the pseudoinverse of the kernel matrix associated with landmark points S . The estimate has several impacts, from both theoretical and practical perspectives. Theoretically, it is the first estimate for the Nyström approximation that works for both SPSD and *indefinite* kernel matrices. The quantities ϵ_1 and ϵ_2 measure the capability of landmark points to capture the geometry of the original dataset and the estimate (1.1) is independent of the particular method to generate the landmark points. Computationally, the error bound

is easy to compute and contains *no* hidden constant. In the context of adaptive algorithms [35], the bound in (1.1) can be used as an a posteriori error estimator with *guaranteed* reliability, meaning that it serves as a strict upper bound of the true error with no implicit multiplicative constant [21, 6, 8].

2. **Improved numerical stability and accuracy.** The Nyström formula requires computing the pseudoinverse of the kernel matrix associated with the landmark points. In some cases, the resulting kernel matrix can be nearly singular, causing numerical instability when computing the pseudoinverse. The issue can be circumvented for SPSD kernels by regularization techniques, i.e., adding a scalar matrix αI with a small constant $\alpha > 0$ to lift all eigenvalues to (α, ∞) and computing the inverse of the sum. For indefinite kernels, however, regularization is no longer effective since the kernel matrix usually has both positive and negative eigenvalues around 0. In this paper, we investigate the impact of landmark points on the numerical rank of the associated kernel matrix. We study for the first time the relation between the data geometry and the numerical rank of the associated kernel matrix. The result implies that increasing the landmark points using methods like uniform sampling or k -means may not help increase the approximation accuracy. We present various experiments to illustrate the breakdown of existing Nyström methods for approximating kernel matrices with rapidly decaying singular values. The new method is shown to have significantly better stability and accuracy.
3. **Deterministic $O(n)$ Nyström method for general symmetric kernels.** Based on the above theoretical results, we leverage the discrepancy theory and propose an efficient deterministic Nyström method for general symmetric kernels. The proposed method does *not* require any access to the kernel matrix or its matrix-vector products in the selection of landmark points and scales $O(n)$ with rigorous theoretical guarantees. Moreover, the proposed method does *not* use over-sampling. It only samples m points from the dataset if a rank- m approximation is sought. On the contrary, probabilistic Nyström methods often need to perform over-sampling in order to achieve the statistical guarantees. For example, for a given approximation accuracy ϵ , $O(m\epsilon^{-2} \ln m)$ data points have to be sampled [2] via uniform sampling or leverage score sampling in order to obtain a rank- m Nyström approximation whose error is bounded by ϵ with certain probability. Since strictly following this sampling strategy makes the algorithm very inefficient, in practice, only $m + O(1)$ points are sampled and thus the assumptions in the statistical guarantee are violated. Finally, we present comprehensive experiments to demonstrate the performance of the proposed method compared to several state-of-the-art methods for various kinds of kernels on both synthetic and real datasets.

The rest of the paper is organized as follows. Section 2 reviews existing Nyström methods for computing low-rank approximations to (SPSD) kernel matrices. Section 3 presents a method-independent Nyström approximation error analysis for general symmetric kernel matrices, covering both SPSD and indefinite ones. In Section 4, we present theoretical results to relate the data geometry to the numerical rank of the kernel matrix. Section 5 introduces the *anchor net method* for computing Nyström approximation. Extensive experiments are provided in Section 6 and concluding remarks are drawn in Section 7.

In the remaining sections, the following notations will be used throughout the paper.

- $|x - y|$ denotes the Euclidean distance between $x, y \in \mathbb{R}^d$;
- $\|\cdot\|$ denotes the 2-norm of a vector or a matrix;
- $\|\cdot\|_{\max}$ denotes the max norm of a matrix, i.e., $\|A\|_{\max} := \max_{i,j} |A_{i,j}|$;
- Let I and J be two finite sets of points in \mathbb{R}^d . We use K_{IJ} to denote a kernel matrix with entries $\kappa(x, y)$ for $x \in I, y \in J$;
- Let $\text{rank}_\epsilon(K)$ denote the ϵ -rank of the matrix K , i.e., the number of singular values that are greater than or equal to ϵ times the largest singular value of K ;
- $\text{dist}_\infty(\cdot, \cdot)$ denotes the distance function in l^∞ norm;
- $\lambda(\Omega)$ denotes the Lebesgue measure of a bounded measurable set Ω in \mathbb{R}^d .

2. Nyström method. Given an input dataset $X = \{x_1, \dots, x_n\} \subset \mathbb{R}^d$ and a symmetric (not necessarily SPSD) kernel function $\kappa(x, y)$, the corresponding kernel matrix is defined by $K = [\kappa(x_i, x_j)]_{i,j=1}^n$. For kernel functions supported on the entire domain of definition, such as $\kappa(x, y) = e^{-\|x-y\|^2}$, the corresponding kernel matrix K is dense and the corresponding cost for storing the matrix or applying it to a vector is $O(n^2)$. Therefore, for large scale datasets, it is favorable in practice to seek a low-rank approximation to K in order to reduce the computational costs.

The Nyström method is an approach developed in the machine learning community to derive the low-rank approximation for SPSD kernel matrices [36]. For an n -by- n SPSD kernel matrix K , it computes a low-rank approximation to K by selecting a subset S with m points ($m \ll n$), which is then used to construct an approximate low-rank factorization in the following form

$$(2.1) \quad K \approx K_{XS} K_{SS}^+ K_{SX},$$

where K_{SS}^+ denotes the pseudoinverse of K_{SS} . The selected points S are called *landmark points*. In almost all Nyström schemes, the set S is constructed as a subset of X . The only exception is the k -means based method [38, 37] where S contains cluster centers which are in general outside X .

Different variants of Nyström methods employ different strategies to choose the landmark points S . The original Nyström method in [36], known as the *uniform* Nyström method, selects landmark points via a uniform sampling over X (or equivalently, over the index set from 1 to n). Since then, a variety of schemes have been developed to select landmark points. See, for example, [38, 19, 37, 20, 1, 14, 26, 32]. Computationally, the uniform Nyström method is the most efficient one, since it does *not* require any access to the kernel matrix or its matrix-vector product, and is not iterative. As a result, the uniform Nyström method is easy to compute and can be applied to a broad class of kernel matrices. The biggest advantage of the uniform Nyström method is that it is free from the curse of dimensionality because the sampling is performed on the index set of the data, independent of the dimension. However, the uniform Nyström method also suffers from several issues. One intrinsic drawback is that, due to the stochastic nature, it suffers from possibly large variance [32]. Another major drawback is that the approximation accuracy usually fails to increase consistently with the increase of the number of landmark points. Experiments show that the accuracy may get stagnated after the number of landmark points goes beyond a certain number. For certain datasets or kernel functions, the uniform Nyström method may even break down (see Section 6).

Non-uniform sampling techniques have been developed to improve the approximation accuracy with strong theoretical guarantees [20, 1, 14, 26]. These methods

measure the importance of each data point with some statistical scores. A notable example is the leverage score based sampling [23, 1, 14]. Each point x_i in the dataset is associated with a leverage score defined as $l_i^\gamma(K) := (K(K + \gamma I)^{-1})_{i,i}$ with $\gamma > 0$ a user-specified parameter. To generate the landmark points, each point x_i is sampled with a probability proportional to $l_i^\gamma(K)$. Since computing leverage scores involves the dense kernel matrix K and computing the matrix inverse $(K + \gamma I)^{-1}$, these methods cost at least $O(n^2)$. Recently, several iterative schemes have been proposed to accelerate its computations [26, 32].

Another variant of Nyström methods is the k -means Nyström method [38, 37]. This method performs the k -means clustering over the dataset and chooses the cluster centers as the landmark points. Similar to uniform sampling, the k -means method does not require any access to the kernel matrix. Experiments show that it tends to be more accurate than the uniform Nyström method [38, 37]. However, as we shall see later in Section 6.2, the k -means Nyström method suffers similar numerical stability issues as uniform sampling when the dataset contains highly unbalanced clusters.

For symmetric *indefinite* kernel matrices, however, it is not clear whether the Nyström approximation in (2.1) is still valid. To the best of our knowledge, no results can be found on applying Nyström method to symmetric indefinite kernel matrices, theoretically and practically. We show in the following sections that Nyström approximation is valid for indefinite kernel matrices but the approximation can be quite unstable if landmark points are not well-chosen. To ensure numerical stability, the impact of the geometry of landmark points on the numerical rank of the kernel matrix is studied in Section 4 and the new method called *anchor net method* is proposed in Section 5 by combining the theoretical findings with the discrepancy theory.

3. Universal error estimates for the Nyström method. In this section, we derive the first universal error bound for the Nyström method. It works for both SPSD and indefinite kernel matrices. It can be applied to *all* variants of the Nyström method as long as the landmark points are chosen from the original dataset. The analysis starts with landmark points without using any information of how they are generated, and the error bound reveals the inherent relation between landmark points and the quality of the corresponding Nyström approximation. It serves as the theoretical foundation of the new method proposed in Section 5.

The lemma below will be used in proving the main result in Theorem 3.2.

LEMMA 3.1. *Assume A is an n -by- n matrix and $\alpha, \hat{\alpha}, \beta, \hat{\beta}$ are n -by-1 vectors. Define $\epsilon_1 := \|\hat{\alpha} - \alpha\|$ and $\epsilon_2 := \|\hat{\beta} - \beta\|$. Then*

$$(3.1) \quad \left| \hat{\alpha}^T A \hat{\beta} - \alpha^T A \beta \right| \leq \|\alpha^T A\| \cdot \epsilon_2 + \|A \beta\| \cdot \epsilon_1 + \|A\| \cdot \epsilon_1 \epsilon_2.$$

Proof. Define $e_1 := \hat{\alpha} - \alpha$ and $e_2 := \hat{\beta} - \beta$. Then (3.1) follows from the fact that

$$\hat{\alpha}^T A \hat{\beta} - \alpha^T A \beta = \alpha^T A e_2 + e_1^T A \beta + e_1^T A e_2.$$

□

In the theorem below, we derive a universal error bound for the Nyström method. The kernel function is assumed to be symmetric and continuous, not necessarily positive-definite. Unlike existing error estimates, the result below is independent of the specific Nyström scheme. The only assumption is that the landmark points belong to the original dataset, which is indeed the case in all Nyström schemes except the one based on k -means clustering [38, 37].

THEOREM 3.2. *Let $\kappa(x, y) \in C(\mathbb{R}^d \times \mathbb{R}^d)$ and $\kappa(x, y) = \kappa(y, x)$. Suppose $X = \{x_1, \dots, x_n\} \subset \mathbb{R}^d$ and $K = K_{XX} := [\kappa(x_i, x_j)]_{i,j=1}^n$. If $S = \{z_1, \dots, z_r\} \subset X$, then*

$$(3.2) \quad \|K - K_{XS}K_{SS}^+K_{XS}^T\|_{\max} \leq E_r + 2\hat{E}_r + \|K_{SS}^+\|\hat{E}_r^2,$$

where

$$(3.3)$$

$$E_r := \max_{x,y \in X} \min_{u,v \in S} |\kappa(x, y) - \kappa(u, v)|, \quad \hat{E}_r := \max_{x \in X} \min_{u \in S} \left(\sum_{i=1}^r |\kappa(x, z_i) - \kappa(u, z_i)|^2 \right)^{\frac{1}{2}}.$$

Proof. Define $R = X \setminus S$. Since $S \subset X$, for some permutation matrix P , there holds

$$K - K_{XS}K_{SS}^+K_{XS}^T = P \begin{bmatrix} O & O \\ O & K_{RR} - K_{RS}K_{SS}^+K_{RS}^T \end{bmatrix} P^T.$$

Consequently, $\|K - K_{XS}K_{SS}^+K_{XS}^T\|_{\max} = \|K_{RR} - K_{RS}K_{SS}^+K_{RS}^T\|_{\max}$. It suffices to estimate the difference below

$$(3.4) \quad \kappa(x, y) - K_{xS}K_{SS}^+K_{yS}^T,$$

where

$$K_{xS} := [\kappa(x, z_1) \ \dots \ \kappa(x, z_r)] \quad \text{for any } x \in \mathbb{R}^d.$$

Note that for any $u, v \in S$,

$$(3.5) \quad \kappa(u, v) = K_{uS}K_{SS}^+K_{vS}^T$$

because $K_{SS}K_{SS}^+K_{SS} = K_{SS}$ and $K_{SS} = K_{SS}^T$. Define the column vectors

$$(3.6) \quad \alpha := K_{uS}^T, \quad \hat{\alpha} := K_{xS}^T, \quad \beta := K_{vS}^T, \quad \hat{\beta} := K_{yS}^T$$

and the scalars

$$(3.7) \quad \begin{aligned} \epsilon_1 &:= \|\hat{\alpha} - \alpha\| = \left(\sum_{i=1}^r |\kappa(x, z_i) - \kappa(u, z_i)|^2 \right)^{\frac{1}{2}}, \\ \epsilon_2 &:= \|\hat{\beta} - \beta\| = \left(\sum_{i=1}^r |\kappa(y, z_i) - \kappa(v, z_i)|^2 \right)^{\frac{1}{2}}. \end{aligned}$$

We can then use (3.5) and (3.6) to rewrite (3.4) as

$$(3.8) \quad \kappa(x, y) - \hat{\alpha}^T K_{SS}^+ \hat{\beta} = (\kappa(x, y) - \kappa(u, v)) + (\alpha^T K_{SS}^+ \beta - \hat{\alpha}^T K_{SS}^+ \hat{\beta}),$$

where $u, v \in S$ can be arbitrary. The second part on the right-hand side of (3.8) can be estimated as follows by using Lemma 3.1:

$$(3.9) \quad \begin{aligned} |\hat{\alpha}^T K_{SS}^+ \hat{\beta} - \alpha^T K_{SS}^+ \beta| &\leq \|\alpha^T K_{SS}^+\| \epsilon_2 + \|K_{SS}^+ \beta\| \epsilon_1 + \|K_{SS}^+\| \epsilon_1 \epsilon_2 \\ &\leq \epsilon_2 + \epsilon_1 + \|K_{SS}^+\| \epsilon_1 \epsilon_2, \end{aligned}$$

where the last inequality is due to the fact that both $\alpha^T K_{SS}^+ = K_{uS}K_{SS}^+$ and $K_{SS}^+ \beta = K_{SS}^+ K_{Sv}$ are row or column of the matrix

$$K_{SS}K_{SS}^+ = K_{SS}^+K_{SS} = U \begin{bmatrix} e_1 & & \\ & \ddots & \\ & & e_r \end{bmatrix} U^T,$$

where U is an orthogonal matrix and $e_i \in \{0, 1\}$, so $\|\alpha^T K_{SS}^+\| \leq 1$ and $\|K_{SS}^+ \beta\| \leq 1$. (3.9) and (3.8) imply the following estimate:

$$(3.10) \quad |\kappa(x, y) - \hat{\alpha}^T K_{SS}^+ \hat{\beta}| \leq |\kappa(x, y) - \kappa(u, v)| + \epsilon_1 + \epsilon_2 + \|K_{SS}^+\| \epsilon_1 \epsilon_2,$$

which holds for any $u, v \in S$. Minimizing the upper bound in (3.10) over all $u, v \in S$ immediately yields

$$(3.11) \quad |\kappa(x, y) - \hat{\alpha}^T K_{SS}^+ \hat{\beta}| \leq \min_{u, v \in S} |\kappa(x, y) - \kappa(u, v)| + \min_{u \in S} \epsilon_1 + \min_{v \in S} \epsilon_2 + \|K_{SS}^+\| \min_{u \in S} \epsilon_1 \cdot \min_{v \in S} \epsilon_2,$$

where ϵ_1, ϵ_2 are defined in (3.7). The proof is completed by taking a maximum of the upper bound in (3.11) over $x, y \in X$. That is,

$$\begin{aligned} |\kappa(x, y) - \hat{\alpha}^T K_{SS}^+ \hat{\beta}| &\leq \max_{x, y \in S} \min_{u, v \in S} |\kappa(x, y) - \kappa(u, v)| + \max_{x \in X} \min_{u \in S} \epsilon_1 + \max_{y \in X} \min_{v \in S} \epsilon_2 \\ &\quad + \|K_{SS}^+\| \max_{x \in X} \min_{u \in S} \epsilon_1 \cdot \max_{y \in Y} \min_{v \in S} \epsilon_2 \\ &= E_r + 2\hat{E}_r + \|K_{SS}^+\| \hat{E}_r^2. \end{aligned} \quad \square$$

Remark 3.3. Note that Theorem 3.2 only requires the kernel function to be continuous and symmetric. Thus the result applies to a broad class of kernels, including SPSD kernels like Gaussian, or more generally Matérn kernels, and indefinite kernels, such as multiquadratics, thin plate spline, Sigmoid kernel, etc. It is the first error analysis of the Nyström approximation that works beyond the scope of SPSD kernels.

We call E_r and \hat{E}_r in Theorem 3.2 the bivariate and univariate *kernelized marking errors*, respectively, as both quantities are measured in terms of either bivariate or univariate kernel function evaluations and indicate the overall capacity of the landmark points S to approximate the dataset X . In view of E_r , we see that the error will be small if for any point $x \in X$, there is a point $u \in S$ nearby. This applies to \hat{E}_r as well. Hence the set of landmark points S is considered good if it is able to minimize the deviation from X , namely, making $\text{dist}(x, S)$ small for each point $x \in X$. In fact, if the kernel function κ is further assumed to be Lipschitz continuous, then we can bound the error by $\max_{x \in X} \text{dist}(x, S)$, as stated in Corollary 3.4.

COROLLARY 3.4. *Under the assumption of Theorem 3.2, if $\kappa(x, y) \in C(\mathbb{R}^d \times \mathbb{R}^d)$ is Lipschitz continuous, i.e., $|\kappa(x', y') - \kappa(x, y)| \leq L(|x - x'|^2 + |y - y'|^2)^{1/2}$ with Lipschitz constant L , then*

$$(3.12) \quad \|K - K_{XS} K_{SS}^+ K_{XS}^T\|_{\max} \leq \sqrt{2}L\delta_{X,S} + 2\sqrt{r}L\delta_{X,S} + \|K_{SS}^+\| rL^2\delta_{X,S}^2,$$

where $\delta_{X,S} = \max_{x \in X} \text{dist}(x, S)$.

Proof. The proof relies on (3.2) and it suffices to relate E_r, \hat{E}_r to $\max_{x \in X} \text{dist}(x, S)$. First we estimate E_r . For each $x \in X$, choose $z_x \in S$ to be the nearest point to x . Then it follows that

$$E_r^2 \leq L^2 \max_{x, y \in X} (|x - z_x|^2 + |y - z_y|^2) = 2L^2 \max_{x \in X} |x - z_x|^2 = 2L^2 \max_{x \in X} \text{dist}(x, S)^2.$$

Similarly, for \hat{E}_r , we deduce that

$$\hat{E}_r^2 \leq L^2 \max_{x \in X} \sum_{i=1}^r |x - z_x|^2 = L^2 \max_{x \in X} r|x - z_x|^2 = rL^2 \max_{x \in X} \text{dist}(x, S)^2.$$

The two estimates and (3.2) immediately imply (3.12) and the proof is complete. \square

Both Theorem 3.2 and Corollary 3.4 justify the use of Nyström approximations for symmetric *indefinite* kernels. They indicate that, theoretically, there should be *no* essential difference between SPSD and indefinite kernels in applying Nyström approximations. This extends the use of Nyström approximation to a significantly wider class of kernels beyond SPSD ones. Compared to the existing error analysis on the Nyström method, the theory developed in this section has the following advantages.

1. **General kernel functions.** Theorem 3.2 only requires the kernel function to be continuous and symmetric, *not* necessarily positive-definite.
2. **Independence of Nyström variants.** Unlike existing error analysis developed for the respective Nyström method, Theorem 3.2 and Corollary 3.4 are independent of the specific Nyström scheme. That is, the estimates in (3.2) and (3.12) can be applied regardless of the particular algorithm (stochastic or deterministic) to generate landmark points.
3. **Deterministic and explicit bound.** The estimates in (3.2) and (3.12) hold true with probability 1 and there is no hidden constant in the error bounds.
4. **Computability.** The estimates in (3.2) and (3.12) are computable and can thus be used to efficiently evaluate the quality of landmark points without computing the actual matrix approximation error.

It can be seen from (3.12) that, to achieve a better approximation, landmark points are encouraged to spread over the entire dataset to capture its geometry, thus reducing $\delta_{X,S}$. Roughly speaking, this means that any point in X is not “too far” from a landmark point in S . In the next section, we will show that this principle also leads to a submatrix K_{SS} with a relatively large numerical rank in general, consequently a numerically more stable computation of K_{SS}^+ compared to matrices with small numerical ranks. If the landmark points S are not well-chosen such that K_{SS} has a small numerical rank, i.e., with most singular values close to 0, then there are two main drawbacks on the resulting Nyström approximation. Firstly, computing K_{SS}^+ will be numerically unstable. Secondly, most singular values of K_{SS}^+ will be quite large, which will yield a large Nyström approximation error according to the estimate in Theorem 3.2.

Remark 3.5. Note also that one may use a different norm to measure the approximation error. The set of optimal landmark points that minimize the error bound may differ, depending on the underlying norm. A detailed investigation on how the norm affects the choice of landmark points will be discussed in a forthcoming paper.

4. Data geometry and numerical rank of the kernel matrix. The error estimates in Theorem 3.2 and Corollary 3.4 indicate that “good” landmark points should be able to capture the geometry of the original dataset in order to reduce the kernelized marking errors E_r and \tilde{E}_r . It is not known, however, the impact of landmark points on K_{SS}^+ , especially the numerical stability when computing K_{SS}^+ . In this section, we show that geometry-aware landmark points will yield a submatrix K_{SS} with a relatively large numerical rank, so that the computation of K_{SS}^+ will be stable and meanwhile $\|K_{SS}^+\|$ will be well bounded. Therefore, the result complements the findings in Section 3 and implies that the numerical stability and the accuracy of the Nyström approximation are in fact interconnected. In order for a Nyström scheme to be effective and efficient for indefinite kernel matrices (which cause more numerical issues than SPSD kernels), the study of numerical stability is of utmost importance.

Due to the appearance of K_{SS}^+ in the Nyström approximation, a major caveat in

selecting the landmark points S is to avoid the submatrix K_{SS} from being (nearly) singular. A nearly singular K_{SS} will cause numerical instability as entries in K_{SS}^+ can be huge. The problem is not addressed in existing literature because the focus has been on SPSD kernels exclusively. For SPSD kernels, one can circumvent this issue by regularization, i.e., replacing K_{SS}^+ with $(K_{SS} + \alpha I)^+$, where $\alpha > 0$ is a small regularization parameter. Unfortunately, for indefinite kernels, regularization techniques may no longer be effective because K_{SS} can have both positive and negative eigenvalues around 0, and $K_{SS} + \alpha I$ can be (nearly) singular even for small values of α . Therefore, it is necessary to investigate systematically the impact of landmark points on the spectral property of K_{SS} and develop a selection scheme such that the resulting submatrix K_{SS} is far from singular. This can be done by studying how the numerical rank of K_{SS} changes as the geometry of landmark points varies. The analysis can also explain the potential breakdowns of uniform sampling as well as k -means in general.

Since the stability issue is common to both SPSD and indefinite kernels, for the ease of analyzing singular values via studying the spectrum, we focus on the SPSD case (singular values coincide with eigenvalues). In fact, since every symmetric matrix can be written as a difference between two SPSD matrices, if the two SPSD matrices are numerically low-rank, then the original matrix is also numerically low-rank. Hence for the sake of convenience, we focus on the SPSD setting to study the spectral property of the kernel matrix. Note that asymptotically, as the number of points in a region goes to infinity, the eigenvalues of the kernel matrix will converge to the spectrum of the integral operator associated with the same kernel, up to a scaling constant [9]. Hence the numerical rank of the kernel matrix is determined by the integral operator and will not grow to infinity as matrix size increases.

In the following, we investigate the effect of data geometries on the numerical rank of the corresponding kernel matrix. To illustrate the idea quantitatively, we take some commonly used radial basis function kernels as examples [7]:

$$(4.1) \quad \begin{aligned} \text{Gaussian: } \kappa(x, y) &= e^{-|x-y|^2/\sigma^2} \\ \text{inverse quadratics: } \kappa(x, y) &= \frac{1}{1 + |x-y|^2/\sigma^2} \\ \text{inverse multiquadric: } \kappa(x, y) &= \frac{1}{\sqrt{1 + |x-y|^2/\sigma^2}}. \end{aligned}$$

We first consider in Theorem 4.1 a simple setting where two datasets differ by only one data point and extend it to more general cases in Corollary 4.2.

THEOREM 4.1. *Let $\kappa(x, y)$ be one of the kernel functions in (4.1). Denote by L the Lipschitz constant of $\kappa(x, y)$. Assume X_0 is a set of $n - 1$ points in \mathbb{R}^d . Let ϵ be an arbitrary number in $(0, 1)$. Consider the following ways of adding a point x^* to X_0 : (1). x^* is close to X_0 with $\text{dist}(x^*, X_0) \leq \epsilon/L$; (2). x^* is away from X_0 with $\text{dist}(x^*, X_0) \geq Q$, where $Q = \sigma\sqrt{|\ln \epsilon|}$ if κ is Gaussian; $Q = \sigma\sqrt{\epsilon^{-1} - 1}$ if κ is inverse quadratic; $Q = \sigma\sqrt{\epsilon^{-2} - 1}$ if κ is inverse multiquadric. Define the $(n - 1)$ -by- $(n - 1)$ kernel matrix $K_0 := [\kappa(x_i, x_j)]_{x_i, x_j \in X_0}$. For case (i), define $K^{(i)}$ to be the n -by- n kernel matrix associated with X_0 and x^* . Then there exist matrices $\tilde{K}^{(1)}$, $\tilde{K}^{(2)}$ such that*

- (1). $\|\tilde{K}^{(1)} - K^{(1)}\| \leq \epsilon\sqrt{n-1}$ and $\text{rank}(\tilde{K}^{(1)}) = \text{rank}(K_0)$;
- (2). $\|\tilde{K}^{(2)} - K^{(2)}\| \leq \epsilon\sqrt{n-1}$ and $\text{rank}(\tilde{K}^{(2)}) = \text{rank}(K_0) + 1$.

Proof. We have

$$K^{(i)} = \begin{bmatrix} K_0 & v_{(i)} \\ v_{(i)}^T & 1 \end{bmatrix},$$

where $v_{(i)}^T = [\kappa(x^*, x_1), \dots, \kappa(x^*, x_{n-1})]$ with x^* in case (i). For case (1), assume without loss of generality that $x_1 \in X_0$ is such that $|x^* - x_1| = \text{dist}(x^*, X_0)$. With $e_1^T = [1, 0, \dots, 0]$, define

$$\tilde{K}^{(1)} := \begin{bmatrix} I \\ e_1^T \end{bmatrix} K_0 \begin{bmatrix} I & e_1 \end{bmatrix} = \begin{bmatrix} K_0 & K_0 e_1 \\ e_1^T K_0 & 1 \end{bmatrix}.$$

For case (2), define $\tilde{K}^{(2)}$ as the n -by- n block diagonal matrix with the first block being K_0 and the second block being 1. Then $\text{rank}(\tilde{K}^{(1)}) = \text{rank}(K_0)$ and $\text{rank}(\tilde{K}^{(2)}) = \text{rank}(K_0) + 1$.

It suffices to prove that $\tilde{K}^{(i)}$ satisfies the estimate $\|\tilde{K}^{(i)} - K^{(i)}\| \leq \epsilon\sqrt{n-1}$, $i = 1, 2$.

First we estimate $\|\tilde{K}^{(1)} - K^{(1)}\|$. According to the definitions of $\tilde{K}^{(1)}$ and $K^{(1)}$, we have

$$\|\tilde{K}^{(1)} - K^{(1)}\| = \|K_0 e_1 - v_{(1)}\| = \left(\sum_{i=1}^{n-1} |\kappa(x_1, x_i) - \kappa(x^*, x_i)|^2 \right)^{1/2}.$$

It follows from the Lipschitz continuity of κ that $|\kappa(x_1, x_i) - \kappa(x^*, x_i)| \leq L|x_1 - x^*|$. Therefore,

$$\|\tilde{K}^{(1)} - K^{(1)}\| = \left(\sum_{i=1}^{n-1} |\kappa(x_1, x_i) - \kappa(x^*, x_i)|^2 \right)^{1/2} \leq L|x^* - x_1|\sqrt{n-1}.$$

Since $|x^* - x_1| = \text{dist}(x^*, X_0) \leq \epsilon/L$, it follows that $\|\tilde{K}^{(1)} - K^{(1)}\| \leq \epsilon\sqrt{n-1}$.

Next consider $\|\tilde{K}^{(2)} - K^{(2)}\|$. We see that $\|\tilde{K}^{(2)} - K^{(2)}\| = \|v_{(2)}\|$. Since $\text{dist}(x^*, X_0) \geq Q$ and $0 < \epsilon < 1$, it can be computed that $\kappa(x^*, x) \leq \epsilon$ for all $x \in X_0$. Consequently, $\|\tilde{K}^{(2)} - K^{(2)}\| = \|v_{(2)}\| \leq \epsilon\sqrt{n-1}$. Now we conclude that $\tilde{K}^{(1)}$ and $\tilde{K}^{(2)}$ are the matrices that satisfy the conditions in the claim and the proof is complete. \square

Theorem 4.1 implies that adding a point away from the original dataset yields a kernel matrix with a larger numerical rank than adding a point close to the dataset. The following corollary generalizes Theorem 4.1 to the case when multiple points are added.

COROLLARY 4.2. *Let X_0 be a set of n points in \mathbb{R}^d and $\epsilon \in (0, 1)$. Consider the following two different distributions of k points with $k \ll n$: (1). Y_1 is a set of k points such that $\max_{y \in Y_1} \text{dist}(y, X_0)$ is small enough; (2). Y_2 is a set of k points such that $\text{dist}(Y_2, X_0)$ is large enough. Define $X_i = X_0 \cup Y_i$ ($i = 1, 2$). Let K_{SS} be the kernel matrix associated with set S . Then*

$$\text{rank}_\epsilon(K_{X_2 X_2}) - \text{rank}_\epsilon(K_{X_1 X_1}) \approx \text{rank}_\epsilon(K_{Y_2 Y_2}).$$

Proof. Since each point in Y_1 is close to X_0 and $k \ll n$, the first case in Theorem 4.1 implies that $\text{rank}_\epsilon(K_{X_1, X_1}) \approx \text{rank}_\epsilon(K_{X_0, X_0})$. Since $\text{dist}(Y_2, X_0) \gg 1$ and $k \ll n$, the second case in Theorem 4.1 implies that $\text{rank}_\epsilon(K_{Y_2, Y_2}) \approx \text{rank}_\epsilon(K_{X_2, X_2})$. Therefore, $\text{rank}_\epsilon(K_{X_2 X_2}) - \text{rank}_\epsilon(K_{X_1 X_1}) \approx \text{rank}_\epsilon(K_{Y_2 Y_2})$.

n , following the same argument as in Theorem 4.1 by redefining $\tilde{K}^{(2)}$ as the block diagonal matrix with diagonal blocks K_{X_0, X_0} and K_{Y_2, Y_2} , we see that

$$\text{rank}_\epsilon(K_{X_2, X_2}) \approx \text{rank}_\epsilon(\tilde{K}^{(2)}) \approx \text{rank}_\epsilon(K_{X_0, X_0}) + \text{rank}_\epsilon(K_{Y_2, Y_2}).$$

Then it follows that $\text{rank}_\epsilon(K_{X_2, X_2}) - \text{rank}_\epsilon(K_{X_1, X_1}) \approx \text{rank}(K_{Y_2, Y_2})$. \square

Theorem 4.1 and Corollary 4.2 imply that if the dataset contains k alienated points outside a dense cluster of n points ($n \gg k$), then compared to sampling m points from the dense cluster, sampling k alienated points and $m - k$ points from the cluster yields a kernel matrix with a larger numerical rank.

In terms of landmark points selection, different schemes generate landmark points S with different shapes, which will affect the spectral property of K_{SS} and consequently the numerical stability in computing K_{SS}^+ . Therefore, to obtain a robust Nyström approximation in practice, it is critical to choose a suitable distribution of landmark points which can yield a kernel matrix with a relatively *large* numerical rank. According to Theorem 4.1 and Corollary 4.2, such a desired distribution of S should capture the geometry of the data without forming clumps, as a clump does not help in increasing the numerical rank of the corresponding kernel matrix.

In general, for highly unbalanced distributions, there is a high probability that the uniform sampling fails to capture the topology of the dataset. Since uniform sampling tends to draw points from the dense clusters, based on Corollary 4.2, we see that the landmark points generated by the uniform Nyström method, denoted by S , will give a submatrix K_{SS} that is not able to capture the numerical rank of the original kernel matrix K . That is, for high-dimensional unbalanced distributions in general, even though enough landmark points are selected, the numerical rank of K_{SS} may be significantly smaller than that of K . In view of the estimate in Theorem 3.2, this will give rise to a large coefficient $\|K_{SS}^+\|$ in the error bound, undermining the quality of the resulting Nyström approximation.

PROPOSITION 4.3. *Let X_1 and X_2 be two disjoint sets with n_1 and n_2 points, respectively. Consider the uniform sampling over the $n_1 + n_2$ points in $X_1 \cup X_2$. If n_2 is fixed, then*

$$\Pr(\text{all } k \text{ samples are in } X_1) \rightarrow 1 \quad \text{as } n_1 \rightarrow \infty.$$

Proof. The probability is equal to $\frac{C_{n_1}^k}{C_{n_1+n_2}^k}$. Hence it can be computed that as $n_1 \rightarrow \infty$,

$$\Pr(\text{all } k \text{ samples are in } X_1) = \frac{1}{1 + \frac{n_2}{n_1}} \cdot \frac{1 - \frac{1}{n_1}}{1 + \frac{n_2-1}{n_1}} \cdots \frac{1 - \frac{k-1}{n_1}}{1 + \frac{n_2-k+1}{n_1}} \rightarrow 1. \quad \square$$

We see from the analysis in this section that, uniform sampling completely ignores the geometry of data and tends to sample landmark points S from dense clusters. According to Corollary 4.2, drawing points from a single cluster as landmark points S does not help to increase the numerical rank of the submatrix K_{SS} . Hence the numerical rank can be much smaller than the size of S , leading to a nearly singular K_{SS} , which will lead to an inaccurate Nyström approximation. This is more likely to happen for unbalanced distributions in high dimensions, as illustrated in Proposition 4.3. In fact, the numerical experiments in Section 6.2 show that, for datasets with highly unbalanced cluster densities, landmark points generated by uniform sampling or k -means may lead to Nyström approximations with no accuracy at all.

The theoretical results in Section 3 and Section 4 show that, in order to obtain an accurate and robust Nyström approximation, the selection of landmark points should respect the overall geometry of the dataset instead of generating a lot more points in denser regions as more landmark points are selected. Based on the theoretical findings, we propose in the next section the anchor net method for the accurate and stable Nyström approximation to general symmetric kernel matrices (both SPSD and indefinite ones).

5. Anchor net method. In this section, we introduce the anchor net method to facilitate the selection of landmark points that ensure a stable and accurate Nyström approximation. From the analysis in Section 3 and Section 4, we see that landmark points that spread evenly in the dataset and contain no clumps are more favorable in reducing the Nyström approximation error. For example, if the dataset is the unit cube, then the uniform grid points satisfy the desired properties. In general, the study of uniformity is a central topic in discrepancy theory. The discrepancy of a given point set measures how far the distribution deviates from the uniform one. In Section 5.1, we review low discrepancy sets, later used as building blocks for the search of good landmark points. Then the anchor net is introduced in Section 5.2. The algorithm for selecting the landmark points is given in Section 5.3, accompanied by a theoretical justification of the method.

5.1. Low discrepancy sets. We start with the concept of low discrepancy sets. Roughly speaking, a dataset with low discrepancy contains points that spread evenly in the space, with almost no local accumulations. There are several kinds of discrepancies [18] and the most widely used one is the star discrepancy, as defined below.

DEFINITION 5.1. *The star discrepancy $D_N^*(\mathcal{A})$ of $\mathcal{A} = \{x_1, \dots, x_N\} \subset [0, 1]^d$ is defined by*

$$D_N^*(\mathcal{A}) := \sup_{J \in \mathcal{J}_1} | \#(\mathcal{A} \cap J) / N - \lambda(J) |,$$

where \mathcal{J}_1 is the family of all boxes in $[0, 1]^d$ of the form $\prod_{i=1}^d [0, a_i]$.

Note that the above definition only applies to datasets in the unit cube.

Low discrepancy sets have been studied in a number of literature as a means of generating quasi-random sequences [17, 33, 25, 18]. The most widely used ones include Halton sequences [17] and digital nets [33, 27, 11]. They are known to have low discrepancies in the sense that $D_N^*(\mathcal{A}_N) = O(N^{-1}(\log N)^d)$, where \mathcal{A}_N denotes the first N terms of the Halton sequence or a digital net [25, 18].

The above low discrepancy sets themselves are inefficient in tessellating a real dataset whose “shape” may not be regular. Therefore, we introduce what we call the *anchor net* in Section 5.2, which is built upon a collection of low discrepancy sets adjusted to the structure of the dataset. Loosely speaking, anchor nets can be viewed as generalized low discrepancy sets dictated by and specific to the given dataset. In order to measure the uniformity of a dataset in a general region, we first generalize Definition 5.1 below.

DEFINITION 5.2. *Let $\mathcal{A} = \{x_1, \dots, x_N\} \subset [0, \infty)^d$ and Ω be a bounded measurable set in $[0, \infty)^d$ such that $\lambda(\Omega) > 0$ and $\mathcal{A} \subset \Omega$. The generalized star discrepancy $D_{N,\Omega}^*(\mathcal{A})$ of \mathcal{A} in Ω is defined by*

$$D_{N,\Omega}^*(\mathcal{A}) = \sup_{J \in \mathcal{J}} | \#(\mathcal{A} \cap J) / N - \lambda(\Omega \cap J) / \lambda(\Omega) |,$$

where \mathcal{J} is the family of all boxes in $[0, \infty)^d$ of the form $\prod_{i=1}^d [0, a_i]$.

Note that the generalized star discrepancy $D_{N,\Omega}^*(\mathcal{A})$ coincides with the standard one $D_N^*(\mathcal{A})$ if $\mathcal{A} \subset \Omega = [0, 1]^d$. If Ω is too large compared to the region occupied by \mathcal{A} , then \mathcal{A} is far from spreading over Ω evenly and we can show that $D_{N,\Omega}^*(\mathcal{A}) \approx 1$ in this case.

5.2. Anchor nets. In this section we first give the formal definition of *anchor net* and then propose an efficient algorithm to construct an anchor net for a given dataset.

DEFINITION 5.3 (Anchor net). *For a dataset $X \subset [0, \infty)^d$, the sets $\mathcal{A}_{X,p} \subset [0, \infty)^d$ of increasing size (in terms of cardinality) parametrized by $p = 0, 1, 2, \dots$ are called anchor nets if the following two conditions are satisfied.*

1. Define $\Omega := \bigcap_{\epsilon > 0} \limsup_{p \rightarrow \infty} \{x \in \mathbb{R}^d : \text{dist}_\infty(x, \mathcal{A}_{X,p}) \leq \epsilon\}$. Then $\lambda(\Omega) > 0$ and $X \subset \Omega$.
2. $\lim_{p \rightarrow \infty} D_{L_p, \Omega}^*(\mathcal{A}_{X,p}) = 0$, where $L_p = \#\mathcal{A}_{X,p}$.

We see that the first condition of Definition 5.3 implies that the anchor net $\mathcal{A}_{X,p}$ becomes dense enough surrounding the given dataset X as p increases and the second condition pertains to the uniformity of the anchor net. As discussed in Section 4, good landmark points are expected to spread over the entire dataset without forming clumps. The anchor net is designed to achieve this goal by leveraging discrepancy theory [27, 11], where one tries to construct low discrepancy sequences (deterministic) in order to avoid clumps that are frequently found in pure random sequences. Low discrepancy sequences can achieve faster convergence than pure random sequences in Monte Carlo methods [28, 25, 11]. Intuitively, one can view the anchor net as the counterpart of low discrepancy sequence and uniform sampling as the counterpart of pure random sequence.

We present an efficient algorithm in Algorithm 5.1 to construct an anchor net that detects the data geometry. In Steps 1 and 11, the choice of the particular low discrepancy set is determined by the user. Options include Halton sequences, digital nets, tensor grids, etc. In Step 11, p_i is a user-defined parameter that indicates the size of $\mathcal{A}_{p_i}^{(i)}$. For example, we can choose $p_i = \#\mathcal{A}_{p_i}^{(i)}$ if $\mathcal{A}_{p_i}^{(i)}$ is a Halton sequence or a digital net, and p_i the sum of the number of nodes in each dimension if $\mathcal{A}_{p_i}^{(i)}$ is a tensor grid. Note that $\#\mathcal{A}_{p_i}^{(i)} = O(1)$ (or $p_i = O(1)$) is independent of n . Theoretically, in order for $\mathcal{A}_{X,p}$ to be an anchor net (cf. Theorem 5.6), p_i is supposed to asymptotically satisfy that

$$(5.1) \quad \lim_{p \rightarrow \infty} \frac{M_i}{\sum_{i=1}^Q M_i} = \frac{\lambda(B_i)}{\sum_{i=1}^Q \lambda(B_i)} \quad \forall i = 1, \dots, Q,$$

where $M_i := \#\mathcal{A}_{p_i}^{(i)}$. Roughly speaking, the condition in (5.1) implies that the size of $\mathcal{A}_{p_i}^{(i)}$ needs to be proportional to the size of B_i , which is a characterization of the natural assumption that more “anchor points” are needed in order to capture larger sets. The size of $\mathcal{A}_{p_i}^{(i)}$ is usually smaller than \mathcal{T} since $\mathcal{A}_{p_i}^{(i)}$ is associated with G_i , a subset of X . One might be tempted to use $\#(B_i \cap X)$ in place of $\lambda(B_i)$ as a guideline for choosing p_i , but it can be computationally more expensive in high dimensions.

Next we prove that $\mathcal{A}_{X,p}$ returned by Algorithm 5.1 is indeed an anchor net. We first prove some lemmas before stating the final result.

Algorithm 5.1 *Anchor net construction*

Input: Given dataset $X = \{x_1, \dots, x_n\} \subset \mathbb{R}^d$ with n data points, integers s and q
Output: Anchor net $\mathcal{A}_{X,p}$

- 1: Create a low discrepancy set $\mathcal{T} = \{t_1, t_2, \dots, t_s\}$ with s points in the smallest box B_0 that contains X
- 2: Initialize $G_i = \{\}$ for $i = 1, 2, \dots, s$.
- 3: **for** $j = 1, 2, \dots, n$ **do**
- 4: Find index i such that $i = \operatorname{argmin}_{k=1, \dots, s} \|x_j - t_k\|_\infty \triangleright \text{Assume } i \text{ is the smallest index}$
- 5: Update $G_i = G_i \cup \{x_j\}$
- 6: **end for**
- 7: Check the number of nonempty G -sets: G_1, \dots, G_Q
- 8: **for** $i = 1, 2, \dots, Q$ **do**
- 9: Find the smallest closed box B_i that contains G_i and compute its Lebesgue measure $\lambda(B_i)$
- 10: **end for**
- 11: Choose Q low discrepancy sets $\mathcal{A}_{p_1}^{(1)} \subset B_1, \dots, \mathcal{A}_{p_Q}^{(Q)} \subset B_Q$ parametrized by p_1, \dots, p_Q such that $p_i \leq q \triangleright p := \min p_i$
- 12: **return** $\mathcal{A}_{X,p} = \bigcup_{i=1}^Q \mathcal{A}_{p_i}^{(i)}$

LEMMA 5.4. For $i = 1, \dots, Q$, define

$$A_\epsilon^{(i)} := \limsup_{p_i \rightarrow \infty} \left\{ x \in \mathbb{R}^d : \operatorname{dist}_\infty(x, \mathcal{A}_{p_i}^{(i)}) \leq \epsilon \right\}.$$

Then $\bigcap_{\epsilon > 0} A_\epsilon^{(i)} = B_i$.

Proof. Without loss of generality, assume $B_i = [0, 1]^d$. Our goal is to prove that $\bigcap_{\epsilon > 0} A_\epsilon^{(i)} = B_i$. It is easy to see that $A_{\epsilon_1}^{(i)} \subset A_{\epsilon_2}^{(i)}$ whenever $\epsilon_1 < \epsilon_2$, so $\bigcap_{\epsilon > 0} A_\epsilon^{(i)}$ can be viewed as the limit of sets as $\epsilon \rightarrow 0$. We first show that $B_i \subset A_\epsilon^{(i)}$ for each $0 < \epsilon < 1$. Fix an $\epsilon \in (0, 1)$. For an arbitrary $x \in B_i$, let J_x be the box centered at x with side ϵ . Define $J = J_x \cap [0, 1]^d$. Then $\lambda(J) \geq (\frac{1}{2})^d \lambda(J_x) = \frac{1}{2^d} \epsilon^d$. Since $\mathcal{A}_{p_i}^{(i)}$ is a low discrepancy set, $D_{M_i}^*(\mathcal{A}_{p_i}^{(i)}) \rightarrow 0$ as $p_i \rightarrow \infty$. Therefore, for the tolerance $\frac{1}{5^d} \epsilon^d$, if p_i is large enough, we have

$$\left| \#(\mathcal{A}_{p_i}^{(i)} \cap J) / M_i - \lambda(J) \right| \leq D_{M_i}^*(\mathcal{A}_{p_i}^{(i)}) < \frac{\epsilon^d}{5^d} < \lambda(J),$$

which implies that $\mathcal{A}_{p_i}^{(i)} \cap J \neq \emptyset$. Hence there is a point in $\mathcal{A}_{p_i}^{(i)}$ whose l^∞ distance to x is within ϵ , i.e.,

$$(5.2) \quad \operatorname{dist}_\infty(x, \mathcal{A}_{p_i}^{(i)}) \leq \epsilon.$$

Note that (5.2) is true as long as p_i is large enough. Consequently, there are infinitely many p_i such that (5.2) holds true. According to the definition of \limsup , it follows that

$$x \in \limsup_{p_i \rightarrow \infty} \left\{ x \in \mathbb{R}^d : \operatorname{dist}_\infty(x, \mathcal{A}_{p_i}^{(i)}) \leq \epsilon \right\} = A_\epsilon^{(i)}.$$

This shows that $B_i \subset A_\epsilon^{(i)}$ since x is arbitrary in B_i . Because $\epsilon > 0$ is arbitrary, we see that $B_i \subset \bigcap_{\epsilon > 0} A_\epsilon^{(i)}$. It remains to prove the other direction: $\bigcap_{\epsilon > 0} A_\epsilon^{(i)} \subset B_i$. This is equivalent to the fact that: if $x \notin B_i$, then $x \notin \bigcap_{\epsilon > 0} A_\epsilon^{(i)}$. Now suppose $x \notin B_i = [0, 1]^d$.

Then $\text{dist}_\infty(x, B_i) = \delta > 0$ for some positive constant δ . We know that $\mathcal{A}_{p_i}^{(i)} \subset B_i$, so $\text{dist}_\infty(x, \mathcal{A}_{p_i}^{(i)}) \geq \delta > 0$ for any p_i . Therefore, $x \notin A_\delta^{(i)}$, which yields that $x \notin \bigcap_{\epsilon > 0} A_\epsilon^{(i)}$.

Now the second direction is proved and we conclude that $\bigcap_{\epsilon > 0} A_\epsilon^{(i)} = B_i$. \square

The next lemma is a property of the generalized discrepancy.

LEMMA 5.5. *Let S_1 and S_2 be two finite subsets of $\Omega_1 \subset [0, \infty)^d$ and $\Omega_2 \subset [0, \infty)^d$, respectively. Suppose $\lambda(\Omega_1 \cap \Omega_2) = 0$ and $S_1 \cap S_2 = \emptyset$. If $D_{N_1, \Omega_1}^*(S_1) < \epsilon$ and $D_{N_2, \Omega_2}^*(S_2) < \epsilon$, where $N_i = \#S_i$, then*

$$(5.3) \quad D_{N_1 + N_2, \Omega_1 \cup \Omega_2}^*(S_1 \cup S_2) < \left| \frac{N_1}{N_1 + N_2} - \frac{\lambda(\Omega_1)}{\lambda(\Omega_1) + \lambda(\Omega_2)} \right| + \epsilon.$$

Proof. Denote $\lambda_i = \lambda(\Omega_i)$ with $i = 1, 2$. Let \mathcal{J} be the family of boxes as in Definition 5.2. For any $J \in \mathcal{J}$, define

$$A_i := \#(S_i \cap J), \quad b_i := \lambda(\Omega_i \cap J), \quad i = 1, 2.$$

According to Definition 5.2 and the assumptions in the claim, it suffices to show that

$$(5.4) \quad \left| \frac{\#((S_1 \cup S_2) \cap J)}{N_1 + N_2} - \frac{\lambda((\Omega_1 \cup \Omega_2) \cap J)}{\lambda(\Omega_1 \cup \Omega_2)} \right| = \left| \frac{A_1 + A_2}{N_1 + N_2} - \frac{b_1 + b_2}{\lambda_1 + \lambda_2} \right| < \left| \frac{N_1}{N_1 + N_2} - \frac{\lambda_1}{\lambda_1 + \lambda_2} \right| + \epsilon.$$

Note first that the definition of $D_{N_i, \Omega_i}^*(S_i)$ yields

$$(5.5) \quad \left| \frac{A_i}{N_i} - \frac{b_i}{\lambda_i} \right| \leq D_{N_i, \Omega_i}^*(S_i) < \epsilon, \quad i = 1, 2.$$

It is easy to see that

$$\begin{aligned} \frac{A_1 + A_2}{N_1 + N_2} - \frac{b_1 + b_2}{\lambda_1 + \lambda_2} &= \frac{N_1}{N_1 + N_2} \cdot \frac{A_1}{N_1} + \frac{N_2}{N_1 + N_2} \cdot \frac{A_2}{N_2} \\ &\quad - \left(\frac{\lambda_1}{\lambda_1 + \lambda_2} \cdot \frac{b_1}{\lambda_1} + \frac{\lambda_2}{\lambda_1 + \lambda_2} \cdot \frac{b_2}{\lambda_2} \right). \end{aligned}$$

Together with (5.5), we deduce that

$$\begin{aligned} &\left| \frac{A_1 + A_2}{N_1 + N_2} - \frac{b_1 + b_2}{\lambda_1 + \lambda_2} \right| < \\ &\left| \left(\frac{N_1}{N_1 + N_2} - \frac{\lambda_1}{\lambda_1 + \lambda_2} \right) \cdot \frac{A_1}{N_1} + \left(\frac{N_2}{N_1 + N_2} - \frac{\lambda_2}{\lambda_1 + \lambda_2} \right) \cdot \frac{A_2}{N_2} \right| + \epsilon \\ &\leq \left| \frac{N_1}{N_1 + N_2} - \frac{\lambda_1}{\lambda_1 + \lambda_2} \right| + \epsilon, \end{aligned}$$

where we have used the fact that $\left| \frac{A_1}{N_1} - \frac{A_2}{N_2} \right| \leq 1$. Since (5.4) is proved for any $J \in \mathcal{J}$, by taking a sup of the left-hand side of (5.4) over $J \in \mathcal{J}$, we conclude that (5.3) holds true. \square

Based on Lemmas 5.4 and 5.5, we next prove that Algorithm 5.1 indeed yields an anchor net.

THEOREM 5.6. $\mathcal{A}_{X,p}$ in Algorithm 5.1 is an anchor net for X .

Proof. We verify that the conditions in Definition 5.3 are satisfied by $\mathcal{A}_{X,p} = \bigcup_{i=1}^Q \mathcal{A}_{p_i}^{(i)}$. The first condition pertains to the set

$$\Omega := \bigcap_{\epsilon > 0} \limsup_{p \rightarrow \infty} \{x \in \mathbb{R}^d : \text{dist}_\infty(x, \mathcal{A}_{X,p}) \leq \epsilon\}.$$

Since $\mathcal{A}_{X,p} = \bigcup_{i=1}^Q \mathcal{A}_{p_i}^{(i)}$, we see that

$$\Omega = \bigcup_{i=1}^Q \bigcap_{\epsilon > 0} \limsup_{p_i \rightarrow \infty} \{x \in \mathbb{R}^d : \text{dist}_\infty(x, \mathcal{A}_{p_i}^{(i)}) \leq \epsilon\} = \bigcup_{i=1}^Q \bigcap_{\epsilon > 0} A_\epsilon^{(i)},$$

where $A_\epsilon^{(i)}$ is defined as in Lemma 5.4. According to Lemma 5.4, it follows that $\Omega = \bigcup_{i=1}^Q B_i$. Consequently,

$$\lambda(\Omega) \geq \lambda(B_1) > 0 \quad \text{and} \quad X \subset \bigcup_{i=1}^Q G_i \subset \bigcup_{i=1}^Q B_i = \Omega,$$

which justifies the first condition in Definition 5.3. Next we prove the second condition:

$$(5.6) \quad \lim_{p \rightarrow \infty} D_{L_p, \Omega}^*(\mathcal{A}_{X,p}) = 0, \quad L_p := \#\mathcal{A}_{X,p}.$$

This is proved by using Lemma 5.5. Assume at this moment $Q = 2$. Then $\mathcal{A}_{X,p} = \mathcal{A}_{p_1}^{(1)} \cup \mathcal{A}_{p_2}^{(2)}$, $\Omega = B_1 \cup B_2$. We deduce from Lemma 5.5 that

$$\lim_{p \rightarrow \infty} D_{L_p, \Omega}^*(\mathcal{A}_{X,p}) \leq \lim_{p \rightarrow \infty} \left| \frac{M_1}{M_1 + M_2} - \frac{\lambda(B_1)}{\lambda(B_1) + \lambda(B_2)} \right| + \lim_{p \rightarrow \infty} \max_{i=1,2} D_{M_i, B_i}^*(\mathcal{A}_{p_i}^{(i)}) = 0,$$

where the first term in the upper bound goes to zero due to (5.1) and the second term vanishes because of the fact that $\lim_{p_i \rightarrow \infty} D_{M_i, B_i}^*(\mathcal{A}_{p_i}^{(i)}) = 0$. If $Q > 2$, based on the result for $Q = 2$, we can apply Lemma 5.5 inductively to show that the condition holds true for $Q = 3, 4, \dots$. Therefore, (5.6) is justified. Now we conclude that the two conditions in Definition 5.3 are both satisfied and thus $\mathcal{A}_{X,p}$ is indeed an anchor net. \square

5.3. Anchor net method. In this section we propose the anchor net method for selecting landmark points and show its optimal property. The anchor net method starts with the construction of an anchor net for the given dataset X and then search for the landmark points in the vicinity of the anchor net. This algorithm is briefly reviewed in Algorithm 5.2. The parameters s and q are $O(1)$, independent of the size of data n and dimension d . In Proposition 5.7, we show that the computational cost of Algorithm 5.2 scales linearly in n .

PROPOSITION 5.7. *Suppose s, q denote the size of \mathcal{T} and the maximum size of $\mathcal{A}_{p_i}^{(i)}$ in Algorithm 5.1, respectively. Then the complexity of the anchor net method described in Algorithm 5.2 is $O(sqdn)$.*

Algorithm 5.2 *Anchor net method*

Input: Given dataset $X = \{x_1, \dots, x_n\} \subset \mathbb{R}^d$ with n data points, integers s and q

Output: The set of landmark points S

- 1: Apply Algorithm 5.1 with parameters s and q to construct the anchor net $\mathcal{A}_{X,p}$ for X
- 2: **for** each point y in $\mathcal{A}_{X,p}$ **do**
- 3: Find x_i s.t., $x_i = \underset{x_k \in X}{\operatorname{argmin}} \|x_k - y\|_\infty$ \triangleright Assume i is the smallest index
- 4: Update $S = S \cup \{x_i\}$
- 5: **end for**
- 6: **return** S

Proof. First we calculate the complexity of Algorithm 5.1. It is easy to see that Step 1 costs $O(sd)$ and the **for** loop in Steps 3–6 amounts to $O(sdn)$.

It can be seen from the **for** loop that $\#G_1 + \dots + \#G_Q = n$. The cost of the **for** loop in Steps 8–10 is then $d \cdot \#G_1 + \dots + d \cdot \#G_Q = dn$. Obviously, the cost of Step 11 is $d \cdot M_1 + \dots + d \cdot M_Q \leq dQ \max_i M_i \leq dQq$, where $M_i := \#\mathcal{A}_{p_i}^{(i)} \leq q$ if q denotes the maximum size of $\mathcal{A}_{p_i}^{(i)}$. Note that $Q \leq s$ because the indices of G -sets in Step 5 of Algorithm 5.1 are associated with points in \mathcal{T} and $\#\mathcal{T} = s$. Overall, we see that the complexity of Algorithm 5.1 is $O(sdn + sdq)$.

Now we are ready to show that the overall complexity of Algorithm 5.2 is optimal. The analysis above for Algorithm 5.1 implies that $\#\mathcal{A}_{X,p} \leq sq$. As a result, the **for** loop in Steps 2–5 of Algorithm 5.2 costs $O(sqn)$. We now conclude that the overall complexity of Algorithm 5.2 is $O(sqn)$. The proof is complete. \square

Remark 5.8. In Proposition 5.7, the assumption that s, q denote the sizes of low discrepancy sets is solely for notational convenience. One can define s, q to be parameters (not necessarily the cardinality) associated with $\mathcal{T}, \mathcal{A}_{p_i}^{(i)}$ and use other notations to replace set sizes s, q in Proposition 5.7. In practice, $s = O(1), q = O(1)$ independent of n , so the complexity in Proposition 5.7 is optimal.

In Theorem 5.9, we show that for highly non-uniform distributions, the anchor net method is able to select much better landmark points than uniform sampling such that the corresponding submatrix K_{SS} has a larger numerical rank.

THEOREM 5.9. *Let $X_1 \subset (0, 1)^d$ be a uniform tensor grid with n_1 points and X_2 be a set of n_2 uniformly distributed points in $\Omega \setminus [0, 1]^d$ for some Ω such that $\operatorname{dist}(X_2, X_1) \gg 1, \operatorname{diam}(X_2) \gg 1$. Let S_0 be the set of k landmark points from the uniform sampling over $X_1 \cup X_2$ and S^* be the set of k landmark points selected via anchor net over $X_1 \cup X_2$. Then as $n_1 \rightarrow \infty$, if k is large enough, with probability approaching 1,*

$$(5.7) \quad \operatorname{rank}_\epsilon(K_{S^*, S^*}) - \operatorname{rank}_\epsilon(K_{S_0, S_0}) \approx \operatorname{rank}_\epsilon(K_{S_2, S_2}), \quad S_2 := S^* \cap X_2.$$

Proof. Define $S_1 := (S_0 \cup S^*) \cap X_1$, the subset of $S_0 \cup S^*$ that is contained in X_1 . According to Proposition 4.3, as $n_1 \rightarrow \infty$, it is almost sure that $S_0 \subset X_1$, which implies that $S_1 = S_0 \cup (S^* \cap X_1)$ and $S_1 \cup S_2 = S_0 \cup S^*$. To prove (5.7), we write $\operatorname{rank}_\epsilon(K_{S^*, S^*}) - \operatorname{rank}_\epsilon(K_{S_0, S_0})$ as the difference

$$(\operatorname{rank}_\epsilon(K_{S^*, S^*}) - \operatorname{rank}_\epsilon(K_{S_1, S_1})) - (\operatorname{rank}_\epsilon(K_{S_1, S_1}) - \operatorname{rank}_\epsilon(K_{S_0, S_0})).$$

First we estimate $\operatorname{rank}_\epsilon(K_{S^*, S^*}) - \operatorname{rank}_\epsilon(K_{S_1, S_1})$. Note that $S^* = (S^* \cap X_1) \cup S_2$,

Table 1: Datasets (n instances in d dimensions)

	Donkey Kong	Abalone	Anuran Calls (MFCC)	Covtype
d	2	8	22	54
n	3000	4177	7195	581012

$S_1 = (S^* \cap X_1) \cup S_0$ and

$$\max_{y \in S_0} \text{dist}(y, (S^* \cap X_1)) \leq \text{diam}(X_1) \ll \text{dist}(S_2, X_1) \leq \text{dist}(S_2, S^* \cap X_1).$$

We see from Corollary 4.2 that $\text{rank}_\epsilon(K_{S^*, S^*}) - \text{rank}_\epsilon(K_{S_1, S_1}) \approx \text{rank}_\epsilon(K_{S_2, S_2})$. Then to prove (5.7), it boils down to showing that $\text{rank}_\epsilon(K_{S_1, S_1}) - \text{rank}_\epsilon(K_{S_0, S_0}) = 0$ when n_1 and k are large enough. In fact, as $n_1 \rightarrow \infty$, $S_0 \subset S_1 \subset X_1 \subset (0, 1)^d$ with probability 1 and both $\text{rank}_\epsilon(K_{S_0, S_0})$ and $\text{rank}_\epsilon(K_{S_1, S_1})$ will converge to the same limit as k increases, since the eigenvalues of those kernel matrices will converge to the eigenvalues of the corresponding integral operator over $(0, 1)^d$ (cf. [3, 9]). This shows that $\text{rank}_\epsilon(K_{S_1, S_1}) = \text{rank}_\epsilon(K_{S_0, S_0})$ if $n_1 \rightarrow \infty$ and k is large enough. The proof is complete. \square

Theorem 5.9 implies that uniform sampling may yield a nearly singular matrix when the dataset is highly irregular while the anchor net method doesn't. In fact, the same drawback is also common to the k -means Nyström method. Since k -means algorithm computes each cluster center as an average of a subset of points, assuming the dataset is highly unbalanced with a lot more points clustered in small regions than widespread ones, as one increases the number of centers (i.e., landmark points), more centers will be created in denser regions of the dataset, leading to the same problem as uniform sampling. The problem is intrinsic to uniform sampling and k -means Nyström methods, since they are based on ideas that fail to address the impact of the selected landmark points on the resulting Nyström approximation accuracy. An example is provided in Section 6.2 to help illustrate the issue.

6. Numerical experiments. In this section we present various experiments to demonstrate the performance of the anchor net method and the numerical instability of some Nyström methods for kernel matrices with rapidly decaying singular values. The datasets are shown in Table 1. All experiments were performed in MATLAB 2020b on a desktop with an Intel i9-9900K 3.60GHz CPU and 64 GB of RAM. The 2-norm is used to measure the Nyström approximation error in all experiments except the one in Figure 7 where 2-norm can not be computed accurately and Frobenius norm is used instead. For probabilistic methods like uniform sampling, the error is averaged over 10 repeated runs, and in each error-rank plot, the solid line corresponds to the averaged error while the dotted line corresponds to the error in an individual run. See, for example, Figures 1 – 3. For the anchor net construction, we choose the low discrepancy set to be the adaptive tensor grid. It's easier to parametrize it using the sum of the number of nodes in each direction. Since each G_i is a subset of X , in Algorithm 5.1, the sizes of $\mathcal{A}_{p_i}^{(i)}$ are in general smaller than \mathcal{T} . In practice, if the pair (a, b) parametrizes the size of \mathcal{T} and the maximum size of $\mathcal{A}_{p_i}^{(i)}$ ($1 \leq i \leq Q$), we can increase the entries in the pair alternatively to refine the anchor net, for example, $(10, 2), (11, 2), (11, 3), (12, 3)$.

6.1. Indefinite kernels. We consider the following indefinite kernels:

$$\begin{aligned} \text{Multiquadratics : } \kappa(x, y) &= \sqrt{|x - y|^2 / \sigma^2 + 1}, \\ \text{Sigmoid : } \kappa(x, y) &= \tanh(x \cdot y / \sigma + 1), \\ \text{Thin plate spline : } \kappa(x, y) &= \frac{|x - y|^2}{\sigma^2} \ln \left(\frac{|x - y|^2}{\sigma^2} \right). \end{aligned}$$

Those kernels are commonly seen in deep learning, kernel density estimation, statistics, etc. To the best of our knowledge, the only Nyström methods that could potentially work for indefinite kernels are the uniform method [36] and the k -means Nyström method [38, 37]. Hence we compare our method to those two. (Note that leverage-score sampling based Nyström methods, such as [12, 14, 26], can not be applied here since they require the kernel matrices to be SPSD.) The k -means method is implemented with an efficient vectorized function to compute L_2 distances between points and centroids at each iteration (Bunschoten, 1999). The iteration number is set to 5. We test the three Nyström methods over the following high-dimensional datasets from the UC Irvine Machine Learning Repository¹: Abalone, Anuran Calls (MFCC), Covertype. See Table 1 for the statistics of the datasets. The datasets are standardized to have zero mean and variance equal to 1. For each kernel, we choose σ to be the half radius of the standardized dataset, where the radius is defined as the maximum distance from a point to the center. The choice ensures that the resulting kernel matrix have fast singular value decay and is thus suitable for low-rank approximations. For the Covertype dataset ($n = 581012$), the Nyström approximation error is evaluated over 10000 randomly sampled points from the dataset.

The error-rank plots in Figures 1 – 3 illustrate how the Nyström approximation error changes as the number of landmark points increases. The computational cost associated with each method is shown in the error-time plots in Figures 4 – 6, where the runtime for each method is computed over ten repeated runs and the approximation error for uniform Nyström method is averaged over ten runs.

We have the following observations regarding the accuracy and stability of the Nyström schemes under comparison for approximating different kinds of *indefinite* kernel matrices.

1. According to Figures 1 – 6, we see that, for different indefinite kernels and datasets, the anchor net method achieves overall the best accuracy for a given approximation rank (i.e., the number of landmark points) and requires little computation time. It is overall more stable than uniform sampling and k -means methods. We also note that the advantage of anchor net method is more prominent for large scale high dimensional datasets like Covertype.
2. Compared to uniform sampling and anchor net methods, the k -means clustering can be quite unstable as one increases the approximation rank, as illustrated in Figures 1-right, 2, 3. This is very likely due to the heuristic and iterative nature of the k -means clustering: the computed cluster centers after a few iterations are unpredictable, and it's hard to know whether the final output can yield a better Nyström approximation accuracy than the initial guess.
3. It's easy to see from Figure 1-right and Figure 2-right that, the anchor net method converges much faster to a fixed accuracy.

¹<https://archive.ics.uci.edu/ml/index.php>

4. For large-scale datasets in high dimensions (e.g. Covertype), the k -means Nyström method is quite slow and is outperformed by uniform sampling according to Figures 4(right) – 6(right).
5. For the Sigmoid kernel with MFCC dataset in Figure 5-middle, all three Nyström schemes display oscillatory behaviors, but the anchor net method stays at a much lower error level, so it actually oscillates with a much smaller amplitude than the other two methods.
6. We see that indefinite kernel matrices are in general much harder for Nyström methods to approximate than SPSD matrices. A possible explanation is that indefinite kernels have more singular values around 0, from both positive side and negative side. As a result, the Nyström approximation is more sensitive to numerical instability. Existing general Nyström schemes (uniform sampling and k -means) can be quite unstable for indefinite kernels, while the anchor net method is very robust and meanwhile achieves better accuracy with less computational cost.

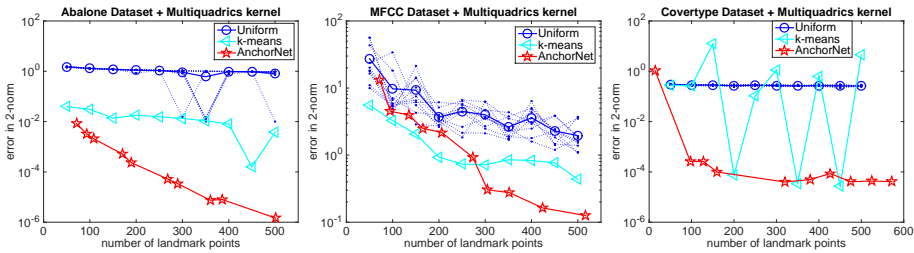


Fig. 1: Multiquadratics: Abalone (left), MFCC (middle), Covertype (right)

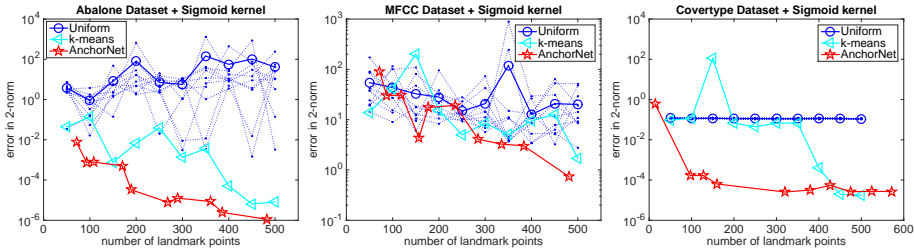


Fig. 2: Sigmoid: Abalone (left), MFCC (middle), Covertype (right)

6.2. Geometry of landmark points and Nyström approximation accuracy. To illustrate how the geometry of landmark points impacts the Nyström approximation, we consider the Sigmoid kernel with $\sigma = 1$ over a highly non-uniform two-dimensional dataset illustrated in Figure 7-left. The singular values of the corresponding kernel matrix decays rapidly, and as a result, Nyström approximation is subject to numerical instability if landmark points are not well-chosen.

In terms of the selection of landmark points, it can be clearly seen from Figure 8 that both uniform sampling and k -means clustering tend to generate more landmark points in denser regions of the dataset, for example, around $(0.4, 0.3)$, $(0.5, 0.7)$, etc. As discussed in Section 4, this does not contribute to a better approximation and,

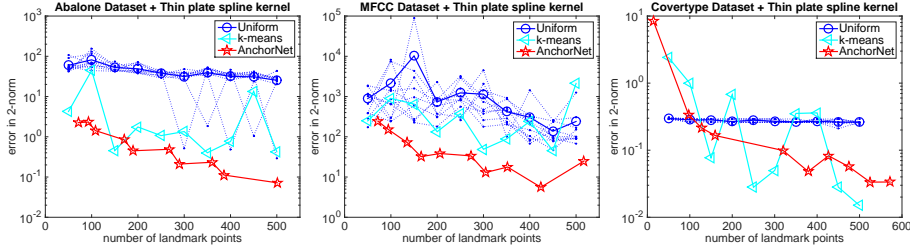


Fig. 3: Thin plate spline: Abalone (left), MFCC (middle), Covertype (right)

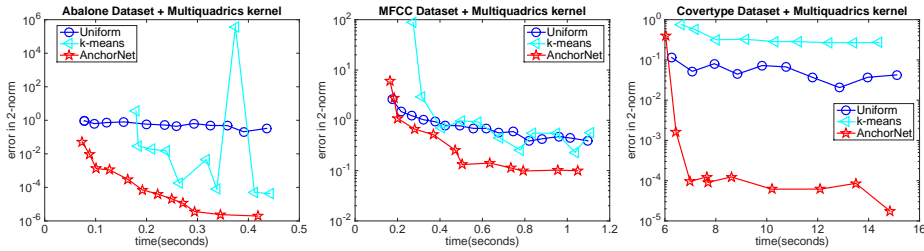


Fig. 4: Multiquadratics Error-Time plot: Abalone (left), MFCC (middle), Covertype (right)

conversely, may lead to numerical instability and possibly a much worse approximation than the one with fewer landmark points.

As reflected in the error plot in Figure 7-right, over ten repeated runs, uniform sampling often becomes ineffective due to the poor choice of landmark points S , which causes the approximation error to blow up when computing K_{SS}^+ . The k -means Nyström method, on the other hand, can sometimes achieve high accuracy when k is small, but becomes quite unstable as k increases. Figure 7-right shows that the k -means Nyström method breaks down when k increases from around 220 to 440. It can be seen that the anchor net method remains robust besides being the most accurate as the number of landmark points increases. Overall, for indefinite kernel matrices and highly non-uniform data, existing Nyström methods tend to generate landmark points that result in an extremely unstable approximation, while the anchor net method is able to yield accurate and robust approximation by choosing geometrically well-balanced landmark points with no clumps. The experiment results justify the theoretical findings in Section 4.

6.3. Numerical stability issues of various Nyström methods. As we have seen from Sections 6.1 and 6.2, one major bottleneck posed by indefinite kernels is the numerical stability of a specific Nyström approximation. Hence in order to successfully apply Nyström method to indefinite kernels, it is essential to ensure that the landmark selection scheme yields a numerically stable approximation. Note that the numerical issue is intrinsic to the Nyström approximation $K \approx K_{XS} K_{SS}^+ K_{SX}$ independent of the positive-definiteness of the kernel: if K_{SS} is nearly singular, computing the pseudoinverse K_{SS}^+ will be numerically unstable. This is unfortunately the case when the Nyström method is used: K has rapidly decaying singular values.

For SPSD kernel matrices, one common strategy employed by many Nyström

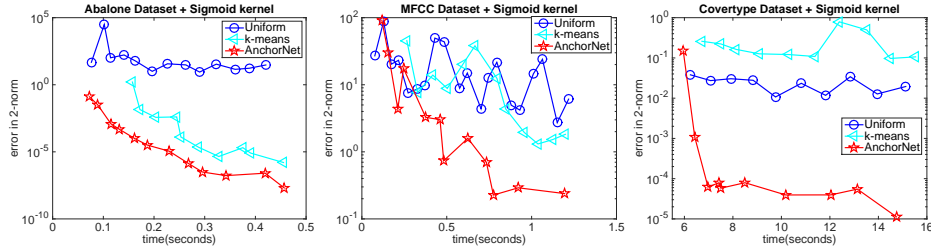


Fig. 5: Sigmoid Error-Time plot: Abalone (left), MFCC (middle), Covertype (right)

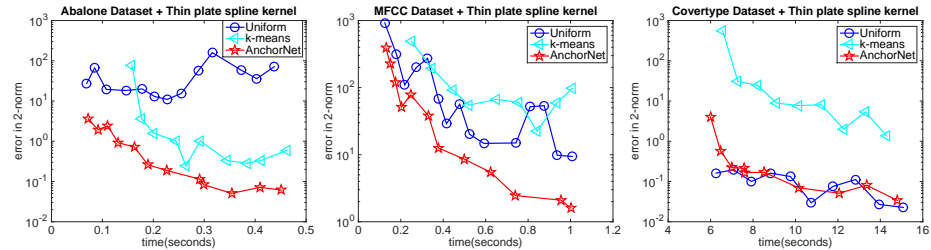


Fig. 6: Thin plate spline Error-Time plot: Abalone (left), MFCC (middle), Covertype (right)

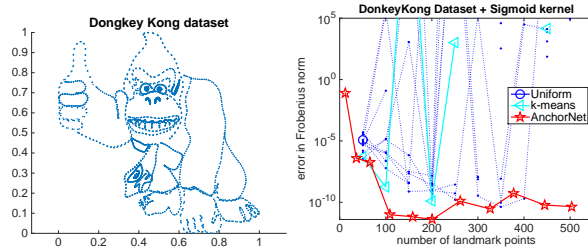


Fig. 7: Left: Donkey Kong dataset; Right: Error-Rank plot for approximating the Sigmoid kernel matrix

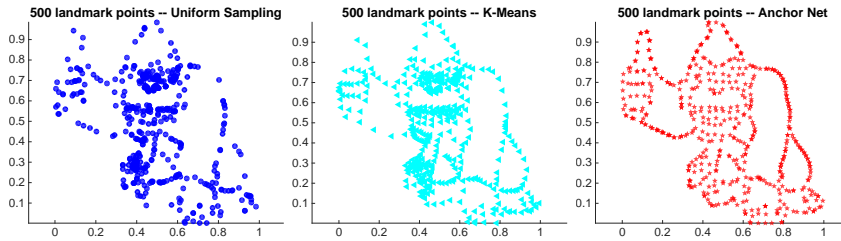


Fig. 8: 500 landmark points generated by: uniform sampling (left), k -means clustering (middle), anchor net method (right). The choices in left and middle yield Nyström approximations with infinitely large errors (see Figure 7).

methods to improve the numerical stability is to use the regularized Nyström approximation $K \approx K_{XS}(K_{SS} + \alpha I)^{-1}K_{SX}$ with $\alpha > 0$ a small regularization parameter. This is because K_{SS} is SPSD, so the eigenvalues (or singular values) of $K_{SS} + \alpha I$ are no smaller than $\alpha > 0$.

However, regularization no longer works in general if K is indefinite, i.e., K has both positive and negative eigenvalues. In this case, $K_{SS} + \alpha I$ will be singular if $-\alpha$ is an eigenvalue of K_{SS} . Hence if a Nyström method breaks down for SPSD kernel matrices without regularization, then it's unrealistic to expect it to work well for indefinite kernel matrices. In case of SPSD kernels, the numerical stability of a Nyström method can be investigated when the original Nyström formula is used (thus without regularization), i.e., $K \approx K_{XS}K_{SS}^+K_{SX}$.

To illustrate the possible numerical instability of existing Nyström methods, we consider the approximation of the Gaussian kernel matrix (which is SPSD) with rapidly decaying singular values. The proposed method (AnchorNet) is compared to the following Nyström schemes: (1) the original uniform Nyström method [36], which was observed in [20] to yield satisfactory overall performance (error-time trade-off) compared to several other methods; (2) the k -means clustering Nyström method [38, 37], which usually yields better accuracy than the uniform Nyström method; (3) the recursive ridge leverage-score (RLS) Nyström method [26], which improves the efficiency of the original leverage-score based sampling; (4) the accelerated recursive ridge leverage-score (RLS-x) Nyström method [26], which is much faster than RLS but may not be as robust. For probabilistic approaches (uniform sampling, RLS, RLS-x), the error is averaged over ten repeated runs.

The methods above are compared from two perspectives: numerical stability and computational efficiency. The Gaussian kernel $\kappa(x, y) = e^{-|x-y|^2/\sigma^2}$ is used and the two experiment settings are listed below.

1. **Numerical stability.** We consider two Gaussian kernels with different choices of the bandwidth parameter σ : 10% and 50% times the radius of the standardized Abalone dataset. Note that larger σ leads to faster singular value decay of the kernel matrix. The results are presented in Figure 9.
2. **Computational efficiency.** We consider two datasets: Abalone ($n = 4177, d = 8$) and Covertype ($n = 581012, d = 54$). For Abalone, we choose $\sigma = 2.3$; for Covertype, σ is same as the one used in Section 6.1. We do not use $\sigma = 11.8$ for Abalone because most methods will be inefficient according to Figure 9. The experiment results are collected as error-time plots in Figure 10. The Covertype dataset is quite large and high-dimensional compared to the Abalone dataset, and the results for the two datasets are quite different, as can be seen in Figure 10.

According to Figure 9 and Figure 10, we have the following observations concerning various Nyström schemes for SPSD kernel matrices.

1. Overall, the anchor net method is more accurate and robust compared to other Nyström methods. It achieves significantly better error-time trade-off for large scale high-dimensional datasets (see Figure 10-right).
2. Figure 9-left and Figure 10-left show that, when the singular values of the Gaussian kernel matrix ($\sigma = 2.3$) do not decay too fast, all methods perform well despite the k -means method being unstable sometimes. The anchor net method achieves better accuracy.
3. As can be seen from Figure 9-middle, for SPSD kernel matrices with rapidly decaying singular values, probabilistic methods, i.e., uniform sampling, recursive leverage score based sampling (RLS) and its accelerated version (RLS-x),

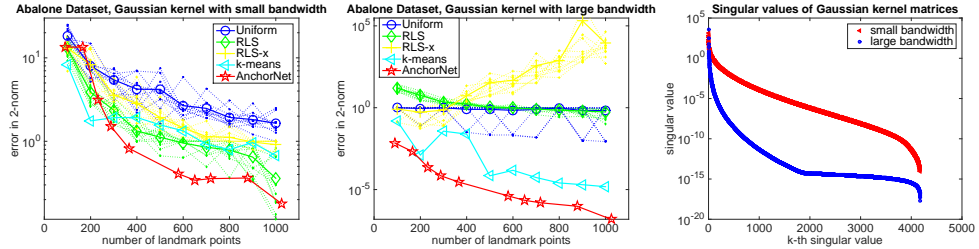


Fig. 9: Error-Rank plot for approximating Gaussian kernel matrix with $\sigma = 2.3$ (left) and $\sigma = 11.8$ (middle) and singular values of the two kernel matrices (right)

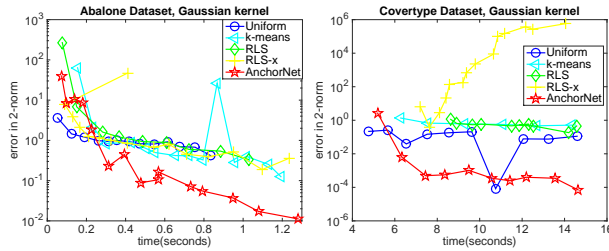


Fig. 10: Error-Time plot for approximating Gaussian kernel matrix with Abalone Dataset (left) and Covertype Dataset (right)

are subject to numerical instability and achieve much lower accuracy than the k -means and anchor net methods. In particular, RLS-x even diverges as the number of landmark points increases. The anchor net method is the most stable one, being able to achieve high accuracy even without regularization.

4. The accelerated RLS (RLS-x) is faster but is less stable than RLS (see Figure 10-right and Figure 9-middle).
5. For large scale high-dimensional datasets like Covertype, we see from Figure 10-right that both k -means and the recursive leverage score (RLS) based Nyström methods become quite slow. The accelerated recursive leverage score method (RLS-x) is initially more efficient than k -means and RLS but then becomes unstable as more landmark points are used. It's easily seen that the anchor net method is the most efficient one, achieving the best accuracy in the shortest time.

Remark 6.1. As shown in Figure 9-right, the kernel matrix with larger σ has faster singular value decay, and consequently is more suitable for low-rank approximations. Nevertheless, it should be emphasized that better spectral property does *not* necessarily imply more accurate Nyström approximations. Instead, it poses a great numerical challenge for the effective use of Nyström approximations: K_{SS} may have many singular values near 0 and computing K_{SS}^+ will be numerically *unstable* unless the landmark points S are wisely chosen. This indicates that the Nyström approximation accuracy can become even worse as the number of landmark points increases. As one can see in Figure 9-middle as well as Figure 7-right, this is indeed the case for many Nyström schemes. The numerical challenge calls for the study in Section 4 on landmark points selection and its impact on the spectrum of the kernel matrix.

7. Conclusion. In this paper, we analyze the Nyström approximation error in the most general setting covering both symmetric positive semi-definite (SPSD) and indefinite kernel matrices. A universal, computable Nyström error estimate is derived for general symmetric kernels and almost all variants of the Nyström method. The results show that indefinite kernel matrices are much harder to approximate numerically than SPSD kernel matrices and existing methods display numerical instability for many kernels and datasets. To address the issues for general symmetric kernels, we justify theoretically that the landmark points should encode the geometry of the dataset to avoid numerical instability and meanwhile to improve the approximation accuracy. Based on the theoretical findings, we introduce the anchor net method. The proposed method is valid for both SPSD and indefinite kernels. Computationally, it operates entirely on the dataset and has the optimal computational complexity. Comprehensive experiments with both indefinite and SPSD kernels are performed to investigate the performance of existing methods in terms of accuracy, numerical stability, and speed. The state-of-the-art probabilistic methods and clustering methods are included in the comparison. The results show that the Nyström method does work for indefinite kernel matrices but is in general numerically less stable compared to approximating SPSD kernel matrices unless the landmark points are wisely chosen. Uniform sampling and k -means Nyström methods can be applied to indefinite kernels but may not yield a satisfactory accuracy. For SPSD kernel matrices with rapidly decaying singular values, probabilistic methods are in general not as numerically stable as k -means and anchor net methods. Overall, for both indefinite and SPSD kernels, the anchor net method displays the best numerical stability. In terms of computational efficiency, the anchor net method is able to achieve better accuracy than other Nyström schemes with smaller computation costs.

REFERENCES

- [1] A. ALAOUI AND M. W. MAHONEY, *Fast randomized kernel ridge regression with statistical guarantees*, in Advances in Neural Information Processing Systems, 2015, pp. 775–783.
- [2] D. ANDERSON, S. DU, M. MAHONEY, C. MELGAARD, K. WU, AND M. GU, *Spectral gap error bounds for improving cur matrix decomposition and the nyström method*, in Artificial Intelligence and Statistics, 2015, pp. 19–27.
- [3] K. E. ATKINSON, *Convergence rates for approximate eigenvalues of compact integral operators*, SIAM Journal on Numerical Analysis, 12 (1975), pp. 213–222.
- [4] F. R. BACH AND M. I. JORDAN, *Kernel independent component analysis*, Journal of machine learning research, 3 (2002), pp. 1–48.
- [5] C. M. BISHOP, *Pattern recognition and machine learning*, Springer, 2006.
- [6] D. BRAESS AND J. SCHÖBERL, *Equilibrated residual error estimator for edge elements*, Mathematics of Computation, 77 (2008), pp. 651–672.
- [7] M. D. BUHmann, *Radial basis functions: theory and implementations*, vol. 12, Cambridge university press, 2003.
- [8] D. CAI, Z. CAI, AND S. ZHANG, *Robust equilibrated a posteriori error estimator for higher order finite element approximations to diffusion problems*, Numerische Mathematik, 144 (2020), pp. 1–21.
- [9] D. CAI AND P. S. VASSILEVSKI, *Eigenvalue problems for exponential-type kernels*, Computational Methods in Applied Mathematics, 20 (2020), pp. 61–78.
- [10] D. DECOSTE AND B. SCHÖLKOPF, *Training invariant support vector machines*, Machine learning, 46 (2002), pp. 161–190.
- [11] J. DICK AND F. PILLICHSHAMMER, *Digital nets and sequences: discrepancy theory and quasi-Monte Carlo integration*, Cambridge University Press, 2010.
- [12] P. DRINEAS AND M. W. MAHONEY, *On the Nyström method for approximating a Gram matrix for improved kernel-based learning*, journal of machine learning research, 6 (2005), pp. 2153–2175.
- [13] B. FORNBERG AND G. WRIGHT, *Stable computation of multiquadric interpolants for all values*

of the shape parameter, Computers & Mathematics with Applications, 48 (2004), pp. 853–867.

- [14] A. GITTENS AND M. W. MAHONEY, *Revisiting the nyström method for improved large-scale machine learning*, The Journal of Machine Learning Research, 17 (2016), pp. 3977–4041.
- [15] B. HAASDONK, *Feature space interpretation of svms with indefinite kernels*, IEEE Transactions on pattern analysis and machine intelligence, 27 (2005), pp. 482–492.
- [16] B. HAASDONK AND D. KEYSERS, *Tangent distance kernels for support vector machines*, in Object recognition supported by user interaction for service robots, vol. 2, IEEE, 2002, pp. 864–868.
- [17] J. H. HALTON, *Algorithm 247: Radical-inverse quasi-random point sequence*, Communications of the ACM, 7 (1964), pp. 701–702.
- [18] L. KUIPERS AND H. NIEDERREITER, *Uniform distribution of sequences*, Courier Corporation, 2012.
- [19] S. KUMAR, M. MOHRI, AND A. TALWALKAR, *On sampling-based approximate spectral decomposition*, in Proceedings of the 26th annual international conference on machine learning, ACM, 2009, pp. 553–560.
- [20] S. KUMAR, M. MOHRI, AND A. TALWALKAR, *Sampling methods for the Nyström method*, Journal of Machine Learning Research, 13 (2012), pp. 981–1006.
- [21] P. LADEVEZE AND D. LEGUILLO, *Error estimate procedure in the finite element method and applications*, SIAM Journal on Numerical Analysis, 20 (1983), pp. 485–509.
- [22] Q. LE, T. SARLÓS, AND A. SMOLA, *Fastfood-approximating kernel expansions in loglinear time*, in Proceedings of the international conference on machine learning, vol. 85, 2013.
- [23] M. W. MAHONEY AND P. DRINEAS, *Cur matrix decompositions for improved data analysis*, Proceedings of the National Academy of Sciences, 106 (2009), pp. 697–702.
- [24] P. MORENO, P. HO, AND N. VASCONCELOS, *A Kullback-Leibler divergence based kernel for SVM classification in multimedia applications*, Advances in neural information processing systems, 16 (2003), pp. 1385–1392.
- [25] W. J. MOROKOFF AND R. E. CAFLISCH, *Quasi-random sequences and their discrepancies*, SIAM Journal on Scientific Computing, 15 (1994), pp. 1251–1279.
- [26] C. MUSCO AND C. MUSCO, *Recursive sampling for the Nyström method*, in Advances in Neural Information Processing Systems, 2017, pp. 3833–3845.
- [27] H. NIEDERREITER, *Point sets and sequences with small discrepancy*, Monatshefte für Mathematik, 104 (1987), pp. 273–337.
- [28] H. NIEDERREITER, *Random number generation and quasi-Monte Carlo methods*, SIAM, 1992.
- [29] C. S. ONG, X. MARY, S. CANU, AND A. J. SMOLA, *Learning with non-positive kernels*, in Proceedings of the twenty-first international conference on Machine learning, 2004, p. 81.
- [30] A. RAHIMI AND B. RECHT, *Random features for large-scale kernel machines*, Advances in neural information processing systems, 20 (2007), pp. 1177–1184.
- [31] A. RAHIMI AND B. RECHT, *Weighted sums of random kitchen sinks: Replacing minimization with randomization in learning*, Advances in neural information processing systems, 21 (2008), pp. 1313–1320.
- [32] A. RUDI, D. CALANDRIELLO, L. CARRATINO, AND L. ROSASCO, *On fast leverage score sampling and optimal learning*, in Advances in Neural Information Processing Systems, 2018, pp. 5672–5682.
- [33] I. M. SOBOL, *Multidimensional quadrature formulas and haar functions*, Izdat. Nauka, Moscow, (1969).
- [34] V. VAPNIK, *The nature of statistical learning theory*, Springer, 2013.
- [35] R. VERFÜRTH, *A Posteriori Error Estimation Techniques for Finite Element Methods*, Numerical Mathematics and Scientific Computation, OUP Oxford, 2013.
- [36] C. K. WILLIAMS AND M. SEEGER, *Using the Nyström method to speed up kernel machines*, in Advances in neural information processing systems, 2001, pp. 682–688.
- [37] K. ZHANG AND J. T. KWOK, *Clustered Nyström method for large scale manifold learning and dimension reduction*, IEEE Transactions on Neural Networks, 21 (2010), pp. 1576–1587.
- [38] K. ZHANG, I. W. TSANG, AND J. T. KWOK, *Improved Nyström low-rank approximation and error analysis*, in Proceedings of the 25th international conference on Machine learning, ACM, 2008, pp. 1232–1239.